Automated Atlas-Based Segmentation of Nissl-Stained Mouse Brain Slices

Olga Senyukova, Alexey Lukin, Dmitry Vetrov*
Department of Computational Mathematics and Cybernetics
Moscow State University, Moscow, Russia
{osenyukova, lukin}@graphics.cs.msu.ru, vetrovd@yandex.ru

Abstract

We introduce a novel automated technique for segmentation of anatomical structures in the images of Nissl-stained histological slices of mouse brain. Segmentation method includes atlas-based supervised learning. An experimental mouse brain slice is preliminarily associated with the corresponding slice from the mouse brain atlas. Then a preprocessing procedure is performed in order to enhance the quality of the experimental image and make it as close to the corresponding atlas image as possible. An effective method of luminance equalization, which is an extension to Retinex algorithm, is proposed.

A supervised learning is performed on the atlas image associated with the experimental slice. A Random Forest is trained on a data derived from the atlas image along with its annotated map, and experimental image pixels are then classified into anatomical structures. The result is refined by Markov random field.

Preprocessing and segmentation procedures have been tested and evaluated on real experimental Nissl-stained slices.

Keywords: *automated segmentation, luminance equalization, Retinex, random forest, Markov random field.*

1. INTRODUCTION

Segmentation of mouse brain images into anatomical structures is a very important problem. It is an essential step of any analysis procedure performed on these images. Manual segmentation turns out to be rather tedious and time-consuming process which requires expert knowledge. Therefore, automated segmentation of mouse brain images is a challenging task.

Fortunately, several publicly available mouse brain atlases exist which can effectively aid the automated segmentation procedure.

Allen Brain Atlas [1] consists of 132 coronal sections evenly spaced at 100 μm intervals and annotated to a detail of numerous brain structures. The images were obtained using Nissl-staining protocol [1] and were manually enhanced using contrast adjustment, etc. Both histological images and corresponding colored annotated maps are presented in the Allen Brain Atlas.

In the present work, we deal with real experimental Nissl-stained slices of mouse brain provided by P. K. Anokhin Institute of Normal Physiology.

Each slice is considered separately. Assuming that for a given experimental slice we know which slice in the atlas it corresponds to, we can use atlas anatomical annotation as a reference. If we put an atlas annotated map directly over the experimental image, it will give a very rough approximation of anatomical structures of the experimental slice because individual local differences in each brain structure's shape and size are not taken into account. Therefore, an annotated map from the atlas should not be used directly for automated segmentation. But, along with this annotated map, a corresponding histological image from the atlas can serve as a labeled training set for supervised learning algorithms for classification of image pixels into anatomical structures. In this work, 17 basic brain structures are considered, such as cerebral cortex, hippocampal formation, thalamus, etc. A Random Forest [2] was chosen as a classification algorithm because it is a fast and highly accurate method which can deal with a very large number of features.

Classification of individual pixels can produce some clutter, especially along the boundaries of anatomical structures. In order to overcome this problem, probabilistic outputs from the random forest are incorporated into Markov random field for further refinement of automated segmentation result.

In order to make the classification algorithm work properly, an experimental image should be preprocessed so that it looks as close to the corresponding atlas image as possible. Preprocessing is always necessary for real experimental images due to non-uniform lighting, low contrast, and other artifacts introduced by the slice image acquisition procedure.

The rest of the paper is organized as follows. An overview of existing mouse brain segmentation methods is given in section 2. Automated preprocessing procedure for experimental images, including luminance equalization, is described in section 3. Automated atlas based segmentation algorithm is described in section 4. Experimental results are presented in section 5. Discussion and conclusion are in section 6.

2. PREVIOUS WORK

Several works devoted to automated mouse brain segmentation exist.

The paper [3] describes a registration scheme to automatically annotate hierarchical brain structures in Nissl-stained mouse brain images using Allen Brain Atlas as a reference. A non-rigid deformation field which best maps the atlas onto the subject image is obtained and it can be used to warp the atlas annotation image thus automatically creating annotations for the subject. Although in our case we know which slice from the atlas an experimental slice corresponds to, differences in shape and size of anatomical structures can be too big for nonlinear warping methods. So, this class of methods can hardly be used for our problem.

A method for segmentation of anatomical structures in histological data is presented in [4]. Segmentation is carried out slice-by-slice by minimizing a cost functional that enforces a compatibility of partitions with corresponding models of region of interest and background (based on intensities and spatial locations) together with the alignment of boundaries with image gradients. This method was designed for segmentation of only one anatomical structure at a time; it does not take into account spatial relations between structures. Therefore it is only suitable for segmentation of anatomical struc-

*This work has been supported by Russian Foundation for Basic Research, project No. 09-04-12215. The authors thank Konstantin Anokhin, Alexander Velizhev and Anton Osokin for a useful discussion.

tures with clear boundaries.

In [5], the classification of voxels in the mouse brain into structures is accomplished by combining magnetic resonance intensity features with spatial priors into a discriminant Bayes classifier. These spatial priors integrate information about the location of structures in the brain as well as the contextual relationship between structures. This contextual information is modeled using the concept of Markov random field (MRF).

The authors of [6] proposed a segmentation method of mouse brain magnetic resonance microscopy (MRM) images that guides the Markov random field clustering with edge information of the MRM images combined with information on the intensity distribution of the various brain structures taken from the atlas.

In [7], authors developed an extended MRF method for automated segmentation of 3D MRM mouse brain images. The eMRF employs the posterior probability distribution obtained from a support vector machine (SVM) to generate a classification based on the MR intensity. To maximize the classification performance, the eMRF uses the contribution weights optimally determined for each of three potential functions: observation, location, and contextual functions, which are traditionally equally weighted.

Magnetic resonance microscopy images of mouse brain differ from Nissl-stained histological images. The latter have a grained, but more accurate pattern. Due to such granulation, classification of individual pixels into anatomical structures based on intensity gives poor results in our case. Nevertheless, the boundaries of anatomical structures are observable. Taking into account that we deal with 2D, not a 3D data, a superpixel-based approach, similar to [8] is introduced in this paper.

3. LUMINANCE EQUALIZATION

Brain slice images obtained from the scanner have very non-uniform illumination (Fig. 1a), which presents a problem for the process of segmentation. A luminance equalization stage of our algorithm restores the luminance uniformity and makes the appearance of the image closer to reference images from the atlas.

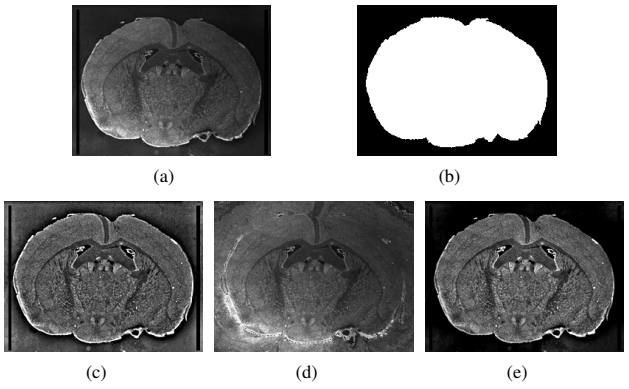

Figure 1: a: raw brain slice image from the scanner; b: brain slice mask; c: retinex algorithm; d: padding of the image outside the slice contour; e: proposed luminance equalization algorithm.

A well-known method for luminance equalization is Retinex [9]. It can be roughly summarized as division of the image by its Gaussian-smoothed copy. The rationale behind the method is that the observed image $Z(x,y)$ can be represented as a product $Z(x,y) = R(x,y)I(x,y)$ of the ground-truth ("reflectance") image $R(x,y)$ and a non-uniform illumination $I(x,y)$. In the absence of accurate information about the illumination image $I(x,y)$, it is estimated as a Gaussian smoothing of the observed image: $I(x,y) = \mathcal{G}(Z(x,y))$. So, $R(x,y)$ is estimated as $R(x,y) = \frac{Z(x,y)}{\mathcal{G}(Z(x,y))}$.

This method has two drawbacks when applied to our problem (Fig. 1c). First of all, since there is an abrupt change of luminance at the boundary contour of the slice, Gaussian smoothing underestimates the luminance of outermost slice pixels. This results in a bright halo at these areas after Retinex. Secondly, Retinex produces visible halos around sharp image edges, for a similar reason.

To address the first problem, we only apply smoothing to the area inside the previously localized brain slice contour (Fig. 1b). Contour localization is performed with EDISON segmentation algorithm [10]. Filtering can be done either by directly constraining Gaussian filter taps to cover the interior area only. But a more computationally effective procedure is possible. We are extending the inner area of the brain slice into the outside (black) area of the image by circular mirroring (Fig. 1d). After that, a fast filtering code that works on the extended rectangular image $E(x,y)$ can be used.

To address the second problem, we have replaced a Gaussian filtering step $\mathcal{G}$ in the Retinex algorithm with a nonlinear kernel. A median filter $\mathcal{M}$ has been chosen for such a nonlinear kernel. Similarly to a multiscale Retinex algorithm [9], we are using 3 median filters of different size $\mathcal{M}_1$, $\mathcal{M}_2$, $\mathcal{M}_3$ in our implementation (whose radii are chosen as 4%, 7%, and 11% of the image width). The resulting formulas for luminance equalization of the extended image are given below:

$$R(x,y) = \frac{E(x,y)}{\mathcal{M}(E(x,y)) + \varepsilon}, \tag{1}$$

$$\mathcal{M}(x,y) = \frac{1}{3}\sum_{i=1}^{3} \mathcal{M}_i(E(x,y)). \tag{2}$$

Here ε (chosen as 2% of peak image brightness) is used to prevent over-amplification of the noise in dark image regions.

The final stage of the process is histogram normalization ("auto-levels" operation). An example of the resulting image can be seen in Fig. 1e.

4. AUTOMATED ATLAS-BASED SEGMENTATION

4.1 Features calculation

As mentioned before, a mouse brain atlas can be used as a labeled training data for classification algorithms. A training set is constructed of a number of training samples. Each sample is a pixel's feature vector along with its label — the ID of the anatomical structure which this pixel belongs to.

This section is devoted to calculation of pixel features. We propose a new combination of features for classification — superpixel features together with location priors for each pixel.

4.1.1 Superpixel features

An individual pixel can only be characterized by three features: (x,y)-position and intensity value. This information is not enough to draw conclusions about its belonging to a particular anatomical structure because a pixel neighborhood is much more informative since it also contains texture information. If we consider an arbitrary neighborhood of the pixel, for example, a square window, it may belong to more than one brain structure in the case when it contains a structure boundary(-ies). Therefore, such pixel neighborhoods cannot serve as training samples — they will confuse a

classifier. Pixel neighborhoods should be image patches ("superpixels") lying inside the boundaries of anatomical structures. Such superpixels are acquired by an extended Mean Shift segmentation algorithm [11]. Then, a set of features is calculated for each superpixel. These features, taken from [12], are divided into 4 categories:

- average color statistics (mean intensity and intensity variance)
- average geometry statistics (square, X-Y covariance, etc.)
- neighborhood statistics (intensity difference with neighboring superpixels)
- sorted color statistics (intensity quantiles).

Each pixel's feature vector is assigned with features of a superpixel it belongs to.

4.1.2 Location priors

Assuming that the experimental slice under consideration is associated with a corresponding slice from the mouse brain atlas, we can assume that its configuration is the same as the atlas slice's one, i.e. the same set of anatomical structures stays in similar positions. Therefore, it is possible to calculate location priors for each pixel $X = (x, y)$ using the atlas annotated map. Location priors is a vector L of prior probabilities of belonging of a pixel (x, y) to each of the anatomical structures:

$$L = [P(a(X) = s_1), P(a(X) = s_2), \ldots, P(a(X) = s_N)], \quad (3)$$

where N is the number of anatomical structures and $a(X)$ is a mapping function from pixels space to anatomical structures labels space.

The idea of location priors was previously used in several works, for example in [5] and [7], but calculation of a probability vector for each spatial location required a training set of several brain instances in order to gather statistics. In our case there is only one brain instance (one slice) so we introduce a new method of calculation of location priors.

The probability of belonging of pixel X to an anatomical structure $s_i, \quad i = 1, \ldots, N$, is calculated as follows:

$$P(a(X) = s_i) = \begin{cases} 1, & a(Y) = s_i, \forall Y \in U(X) \\ 0, & \forall Y \in U(X) \nexists Y : a(Y) = s_i \\ 0.5, & \exists Y_1 : a(Y_1) = s_i \wedge \exists Y_2 : a(Y_2) \neq s_i, \\ & Y_1, Y_2 \in U(X) \end{cases} \quad (4)$$

$U(X) = \{Y : |Y - X| \leq R\}$, i.e. $U(X)$ is a circular neighborhood of X with radius R.

4.1.3 Construction of a feature vector

The final feature vector for each pixel is constructed by concatenation of superpixel features and location priors.

4.2 Classification of pixels

Random forest is a combination of tree predictors, such that each tree depends on the values of a random vector of training samples taken independently and with the same distribution for all trees in the forest. Random forest outputs the class that is the mode of the class outputs by individual trees. An output from this classifier for a sample X can be represented in a probabilistic form, similar to (3):

$$C = [P(a(X) = s_1), P(a(X) = s_2), \ldots, P(a(X) = s_N)], \quad (5)$$

where

$$P(a(X) = s_i) = \frac{N_{trees} : a(X) = s_i}{N_{trees}}, \quad i = 1, \ldots, N. \quad (6)$$

So, after random forest classification for each pixel we can obtain a vector of probabilities of its belonging to each of the anatomical structures.

4.3 Incorporation of the classifier output into MRF

Classification of individual pixels can produce some noise, especially near the boundaries of anatomical structures, because it does not take into account spatial relations between pixels. Introduction of Markov random field can effectively address this problem. An image can be described by a Markov network where x_j are observable variables — pixels, and t_j are latent variables — their labels.

The most probable values of latent variables are reconstructed from observable variables:

$$T_{MP} = \arg\max_T P(T|X) \quad (7)$$

The problem of finding the most probable distribution can be reduced to energy minimization problem:

$$E(T|X) = \sum_{(i,j)\in E} E_{ij}(t_i, t_j) + \sum_i E_i(x_i, t_i) \to \min_T, \quad t_i \in \{1, \ldots, N\} \quad (8)$$

Minimization of energy by k-valued latent variables is an NP problem, nevertheless it is possible to construct an iterative procedure which approximately converges to a global optimum.

Unary term in (8) stands for a correspondence of the pixel with each of the classes. In our case it is calculated as follows:

$$E(x, t) = -\log_{10} C, \quad (9)$$

where C is the random forest output from equation (5).

Binary term in (8) reflects correlation between classes of neighboring pixels. In the present work, Potts model is used where non-coincidence of neighboring pixel classes is penalized by a constant value of 1:

$$E_{ij}(t_i, t_j) = 1 - \delta(t_i, t_j) \quad (10)$$

5. EXPERIMENTS

The described atlas-based segmentation algorithm was tested on real experimental Nissl-stained mouse brain slice images preprocessed by the proposed luminance equalization method. Results are shown in Fig. 2. It can be seen that introduction of MRF is necessary to make anatomical structures continuous.

Implementation details are given below.

Brain slice image size is 270×204 pixels. During random forest classification each pixel was represented by a vector of 75 superpixel features and 17 location priors corresponding to 17 anatomical structures. Radius of the location prior is equal to 8 pixels. Random forest classifier was constructed of 100 trees with the maximum depth of 30.

The proposed segmentation algorithm was evaluated on 10 pairs of neighboring slices from the Allen Brain Atlas. One slice from each pair was used for training and the other one, its neighbor, for testing. Pairs of slices were taken randomly from different parts of the Allen Brain Atlas. Overall precision and precision per structure averaged from 10 different pairs are presented in Table 1.

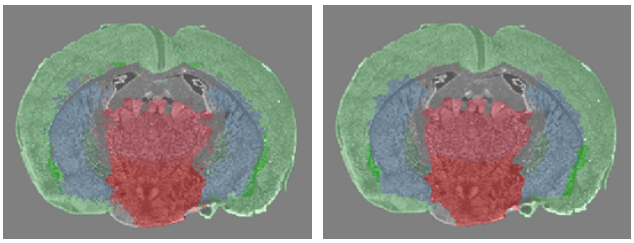

(a) (b)

Figure 2: a: segmentation result after pixel classification with random forest; b: segmentation result after MRF refinement.

Table 1: Precision

Overall	CBy	FT	G	CBv
0.860589	0.902196	0.568939	0.500531	0.921488
MY	MB	P	CLXg	6b
0.764072	0.948688	0.816145	0.929592	0.309266
HPFg	HPF	TH	HY	STR
0.905144	0.607194	0.952606	0.867327	0.949691
PAL	CLXv			
0.616833	0.738971			

Precision was calculated as follows. First of all, the confusion matrix for each pair of slices was calculated. It is a square matrix M whose elements m_{ij} reflect the number of pixels of i-th true anatomical structure that were (mis-)classified as j-th anatomical structure during the automated segmentation procedure. Ideally, M is a diagonal matrix, which means that all the pixels were correctly annotated. Precision for i-th anatomical structure is calculated by the formula:

$$p_i = \frac{m_{ii}}{\sum_j m_{ij}} \tag{11}$$

Overall precision for a pair of slices is calculated by the formula:

$$p = \frac{\sum_i m_{ii}}{\sum_{i,j} m_{ij}} \tag{12}$$

6. CONCLUSION AND DISCUSSION

We have proposed a method for automatic atlas-based segmentation of Nissl-stained mouse brain slice images which takes into account texture peculiarities of images obtained by this protocol. An effective technique for luminance equalization was introduced. It significantly enhances the quality of real experimental images and makes them close to Allen Brain Atlas images, which is essential for segmentation based on supervised learning.

A novel segmentation framework is introduced. Visual analysis and numerical results show that the algorithm performs rather well on large anatomical structures such as cerebral cortex *(CLXg)*, thalamus *(TH)*, etc. Thin and small structures, especially with fuzzy boundaries, such as *6b* are difficult to segment. Classification errors can occur across the boundaries of anatomical structures in cases when these boundaries are not clear or when a boundary between structures lies far from the corresponding boundary on the training brain slice. Similar problems are discussed in previous works devoted to automated segmentation of MRM brain volumes. Numerical results represented in Table 1 are comparable to those from previous works.

In the future, we will add textons (texture elements) to feature vectors in order to include local texture information, which is probably helpful for classification of anatomical structures. Shape priors will also be incorporated into the automated segmentation framework.

7. REFERENCES

[1] Allen Brain Atlas

http://mouse.brain-map.org/atlas/index.html

[2] Leo Breiman, "Random Forests," *Machine Learning*, vol. 45, no. 1, pp. 5–32, 2004.

[3] Lydia Ng, Michael Hawrylycz, and David Haynor, "Automated high-throughput registration for localizing 3D mouse brain gene expression using ITK," *Insight Jounral*, vol. 1, 2005.

[4] T. Riklin-Raviv, N. Sochenz, N. Kiryati, N. Ben-Zadok, S. Gefen, L. Bertand and J. Nissanov, "Propagating Distributions for Segmentation of Brain Atlas," *4th IEEE International Symposium on Biomedical Imaging: From Nano to Macro*, pp. 1304–1307.

[5] Anjum Ali, Anders Dale, Alexandra Badea and Allan Johnson, "Automated Segmentation of Neuroanatomical Structures in Multispectral MR Microscopy of the Mouse Brain," *Neuroimage*, vol. 27, no. 2, pp. 425–435, 2005.

[6] Alize Scheenstra, Jouke Dijkstraa, Rob van de Ven, Louise van der Weerd and Johan Reiber, "Automated Segmentation of the Ex Vivo Mouse Brain," *Proceedings of the SPIE*, vol. 6511, pp. 651106, 2007.

[7] Min Bae, Rong Pan, Teresa Wu and Alexandra Badea, "Automated Segmentation of Mouse Brain Images Using Extended MRF," *Neuroimage*, vol. 46, no. 3, pp. 717–725, 2009.

[8] Brian Fulkerson, Andrea Vedaldi and Stefano Soatto, "Class Segmentation and Object Localization with Superpixel Neighborhoods," *International Conference on Computer Vision*, pp. 670–677, 2009.

[9] Z. Rahman, D. Jobson and G. A. Woodell, "Multiscale Retinex for color image enhancement," *Proceedings of the IEEE Int. Conf. In Image Processing*, pp. 1003–1006, 1996.

[10] Christopher Christoudias, Bogdan Georgescu and Peter Meer, "Synergism in Low Level Vision," *International Conference on Pattern Recognition*, vol. 4, pp. 150–155, 2002.

[11] Sylvain Paris and Fredo Durand, "Topological Approach to Hierarchical Segmentation using Mean Shift," *IEEE Conference on Computer Vision and Pattern Recognition*, pp. 1–8, 2007.

[12] Sergey Sudakov, Olga Barinova, Alexander Velizhev and Anton Konushin, "Semantic segmentation of road images based on cascade classifiers," *Proceedings of the ISPRS XXI Congress*, pp. 601–604, 2008.

ABOUT THE AUTHORS

Olga Senyukova is a Ph.D. student at Graphics & Media Lab within the Moscow State University's CMC Department.
Her contact email is osenyukova@graphics.cs.msu.ru

Alexey Lukin, Ph.D., is a member of scientific staff at the Laboratory of Mathematical Methods of Image Processing within the Moscow State University's CMC Department.
His contact email is lukin@graphics.cs.msu.ru

Dmitry Vetrov, Ph.D., is a member of scientific staff at the Chair of Mathematical Methods of Forecasting within the Moscow State University's CMC Department.
His contact email is vetrovd@yandex.ru